Non-Coherent Cell Identification Detection Methods and Statistical Analysis for OFDM Systems

Chih-Liang Chen and Sau-Gee Chen

***Abstract*—To achieve high-performance cell identification detection with low complexity for orthogonal frequency division multiplexing (OFDM) systems, this work proposes an efficient non-coherent cell identification (ID) detection technique based on a new optimization metric. Furthermore, the metric is simplified to two lower-complexity metrics. As such, two more modified cell ID detection methods extended from the first one are also proposed. Experiments show that all the three new cell ID methods achieve better performances than the conventional methods in multipath Rayleigh fading channels. This work also conducts the statistical analysis to characterize the proposed techniques completely. It is shown that the results of the theoretical analysis are close to the simulation results. Among the new techniques, specifically, the third proposed method using the second simplified new metric has much lower complexity and higher performance than the conventional methods.**

***Index Terms*—Orthogonal frequency division multiplexing (OFDM), cell identification, cell identification detection, multipath fading channel.**

I. Introduction

SINCE the recent decade, the demand for portable devices with wireless real-time and high-rate multimedia services has been in a rapid growing pace. To meet the demand, the cellular orthogonal frequency division multiplexing (OFDM) system is widely adopted by many current and next-generation wireless communication specifications, including the IEEE 802.16e, 802.16m and 3GPP LTE systems. In a cellular OFDM system, a serial data stream is split into several parallel data streams. Then, each parallel data stream modulates its corresponding subcarrier which is orthogonal to all the other subcarriers. Thus, for each subcarrier, OFDM technique transforms the frequency-selective fading channel into many flat-fading subchannels. This feature significantly simplifies the equalizer designs. Besides, by adding a cyclic prefix (CP) to the beginning of each OFDM symbol, the intersymbol interference (ISI) caused by the channel delay spread can be reduced and the subcarrier orthogonality can be maintained.

When a mobile station (MS) wants to access a cellular OFDM system, it needs to know the cell identification (ID) information of the cell it resides. In most existing systems (for example, IEEE 802.16e/j), non-hierarchical preamble structures [2][3] with a large number of cell-specific sequences are adopted. In this work, we also assume the non-hierarchical structure. To obtain the cell ID involves complicated and computational intensive matching operations. Hence, for the consideration of low access delay and low complexity, a highly efficient and accurate cell ID detection process is required to find out the index of the transmitted preamble.

There are two kinds of cell ID detection methods, namely coherent and non-coherent methods, for cellular OFDM systems in the literature. Coherent cell ID detection methods [3][4][5][6] require channel information, while non-coherent cell ID detection methods [7][8][9][10][11] do not. For practical systems, normally initial synchronization processes including the cell identification are conducted first, followed by the process of channel estimation. That is, non-coherent methods are mostly adopted by current communication systems. As such, this work assumes non-coherent cell ID detection and focuses on improving the performances of the non-coherent cell ID detection methods. For IEEE 802.16e OFDM system [13][14], the cell ID detection method [7] is based on an autocorrelation technique. The autocorrelation technique determines the cell ID by detecting the maximum value of all the correlation values between the received frequency-domain signal and all the reference preamble signals. In [22], authors propose two frame detection methods (namely TD and FD) and combine those methods with adaptive correlation length (ACL). With shorter correlation length, [22] can reduce the computational complexity during the cell ID identification stage. However, note that [22] still utilizes the conventional correlation procedure during the cell ID identification stage. Thus, it is a simplified autocorrelation method.

However, in multipath fading channel environments, the frequency-domain correlation is likely influenced by frequency selective fading. As such, differential demodulation is employed prior to the autocorrelation for mitigating the frequency selective fading. In fact, most of the existing non-coherent cell ID methods [8][9][10][11] for cellular OFDM systems are based on the differential autocorrelation technique. Hence, this work will directly compare the performance and complexity between the proposed methods and the differential autocorrelation technique. Although the differential autocorrelation technique has high performance, the most critical disadvantage of the differential autocorrelation technique is that it requires a large number of complex multiplication operations. For example, since there are 114 sets of known reference preambles in IEEE 802.16 and IEEE 802.16e OFDM systems, the involved computation complexity is enormous for those autocorrelation-based methods. Beside, a technique in [21], called the code group identification method, detects the code group ID by dividing the received signal into four non-overlapping parts.

Paper approved by E. Perrins, the Editor for Modulation Theory of the IEEE Communications Society. Manuscript received August 12, 2009; revised April 19, 2010 and June 19, 2010.

Parts of this work have been presented at the IEEE Personal, Indoor and Mobile Radio Communications (PIMRC) Conference, 2008.

The authors are with the Department of Electronics Engineering and Institute of Electronics, National Chiao Tung University, 1001 University Road, Hsinchu, Taiwan (e-mail: clchen.nctu@gmail.com; sgchen@mail.nctu.edu.tw).

Digital Object Identifier 10.1109/TCOMM.2010.091710.090472

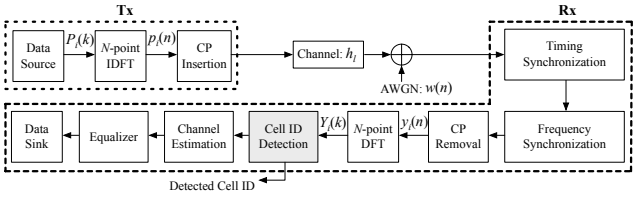

Fig. 1. Simplified discrete-time OFDM system structure.

The method will achieve good integration gain if the channel variation is small or the channel response is flat, otherwise the integration gain will be low if the channel variation is large or the channel response is highly frequency selective. Therefore, in that case, it will misdetect the preamble sequence.

To significantly reduce the complexity and achieve high performance at the same time, this paper proposes three efficient non-coherent cell ID detection methods based on a new optimization metric and its simplifications. These new methods are not only suitable for IEEE 802.16 and IEEE 802.16e systems but also suitable for other preamble-based OFDM systems. By combining a preamble matching process and a multiplication-free smoothing scheme, the proposed techniques achieve better performances than the existing techniques in multipath Rayleigh fading channels. Based on our preliminary work [1], which introduces a basic concept of smoothing for cell ID detection, this paper generalizes the design concept and provide a statistical characterization for the proposed methods. Moreover, for further reducing the complexity, we introduce the decimation factor d into the conventional and proposed methods as shown in the section of simulation results. With the decimation, all the methods can achieve lower computational complexities. For a system suffering the burst error, reducing the complexity by decimation may be better than reducing the complexity by directly shortening the correlation length in [22]. Therefore, by appropriately choosing the value of decimation factor d, the proposed methods can achieve the similar complexities as [22], but with better system performances.

The rest of this paper is organized as follows. Section II describes the OFDM system model and the differential autocorrelation technique adopted by conventional cell ID detection methods. Section III introduces the proposed cell ID detection methods based on three new optimization metrics. In Section IV, theoretical analysis of the proposed optimization metric is conducted which includes the mean value analysis and the lower bound analysis of the variance. Section V provides the computational complexity analysis of the conventional and the proposed methods. Simulation results in different channel conditions are presented in Section VI. Finally, Section VII is the conclusion.

II. OFDM System Model and Conventional Differential Autocorrelation Technique

A. OFDM System Model

Fig. 1 shows a simplified discrete-time OFDM system structure, where N is the total number of subcarriers. For cell identification, it is assumed that the system is transmitting a specific preamble signal $P_i(k)$, $0 \le k \le N-1$, where i and k are the preamble index and subcarrier index, respectively. This work assumes that the transmitted preamble is BPSK-modulated pseudo-noise (PN) code (as defined in IEEE 802.16e standard) and the total number of the known reference preambles is M. In the cell ID detection process, $P_i(k)$ is to be identified from the set of all the possible reference preambles $P_m(k)$, $0 \le m \le M-1$. The modulators in the transmitter and the matched filters in the receiver for the OFDM systems can be implemented by IDFT and DFT [12], respectively. The signal after IDFT is

$$p_i(n) = \frac{1}{N}\sum_{k=0}^{N-1} P_i(k) e^{\frac{j2\pi kn}{N}},\ 0 \le n \le N-1. \quad (1)$$

The signal is then preceded with a CP and delivered through a time-invariant Rayleigh fading channel. The channel paths h_l, $0 \le l \le L-1$, are assumed uncorrelated zero-mean complex Gaussian random variables with variance $\sigma_{h_l}^2$, where L is the total number of channel paths. After the timing synchronization and frequency synchronization, the timing and frequency offset can be compensated. Therefore, the received signal can be represented as

$$y(n) = \sum_{l=0}^{L-1} h_l p_i(n-l)_N + w(n), \quad (2)$$

where $(\cdot)_N$ represents the modulo N operation and $w(n)$ is a zero-mean additive white complex Gaussian noise (AWGN) with variance σ_w^2. The received signal after DFT at the k-th subcarrier is

$$Y(k) = \sum_{n=0}^{N-1} y(n) e^{-\frac{j2\pi kn}{N}}. \quad (3)$$

By substituting (1) and (2) into (3), the k-th subcarrier signal $Y(k)$ is

$$Y(k) = H(k)P_i(k) + W(k), \quad (4)$$

where $H(k)$ is the channel frequency response at the k-th subcarrier, namely,

$$H(k) = \sum_{l=0}^{L-1} h_l e^{\frac{-j2\pi lk}{N}},\ 0 \le k \le N-1,$$

and $W(k)$ is the DFT of the zero-mean AWGN $w(n)$, i.e.,

$$W(k) = \sum_{n=0}^{N-1} w(n) e^{\frac{-j2\pi kn}{N}},\ 0 \le k \le N-1.$$

Note that since the channel paths h_l and AWGN $w(n)$ are complex Gaussian random variables, $H(k)$ and $W(k)$ are also complex Gaussian random variables.

Although timing synchronization and frequency synchronization are performed before the cell ID identification stage, residual timing error τ and residual frequency offset ϵ may still exist. As such, for a complete system modeling, (4) can be further revised [19][20] as

$$Y(k) = H(k)P_i(k)L(k) + I(k) + W(k)e^{j\frac{-2\pi k\tau}{N}}, \quad (5)$$

where

$$L(k) \equiv \frac{\sin(\pi\epsilon)}{N\sin(\frac{\pi\epsilon}{N})} e^{j\frac{\pi(N\epsilon-\epsilon-2k\tau)}{N}},$$

and $I(k)$ is inter-carrier interference (ICI) caused by the frequency offset and represented as

$$\begin{aligned} I(k) &\equiv \textstyle\sum_{m=0,m\neq k}^{N-1} H(m)P_i(m) \times \frac{\sin(\pi(\epsilon+k-m))}{N\sin(\frac{\pi(\epsilon+k-m)}{N})} \\ &\quad \times e^{j\frac{\pi(\epsilon+k-m)(N-1)}{N}} e^{j\frac{-2\pi k\tau}{N}}. \end{aligned}$$

Note that the channel paths and AWGN are complex Gaussian random variables, and are also complex Gaussian random variables. The next step is to recognize the transmitted preamble index (i.e., cell ID) from all the possible preambles.

B. Conventional Differential Autocorrelation Technique

Basically, the conventional differential autocorrelation technique [8][9][10][11] can be represented as

$$\hat{i} = \arg \max_{0\leq m\leq M-1} \sum_{k=0}^{N-2} Y(k)Y^*(k+1)P_m(k)P_m(k+1), \tag{6}$$

where $\hat{i}$ is the detected cell ID. For explaining the idea of the conventional technique, the discussion starts with the following preamble matching operation at the k-th subcarrier:

$$\begin{aligned} M_{i,m}(k) &= Y(k)P_m(k) \\ &= H(k)P_i(k)P_m(k)L(k) + I(k)P_m(k) \\ &\quad + W(k)P_m(k)e^{j\frac{-2\pi k\tau}{N}} \\ &= H(k)X_{i,m}(k)L(k) + I(k)P_m(k) \\ &\quad + W(k)P_m(k)e^{j\frac{-2\pi k\tau}{N}}, \end{aligned} \tag{7}$$

where

$$X_{i,m}(k) \equiv P_i(k)P_m(k).$$

Because of the BPSK-modulated preambles, there are only two possible outcomes of $X_{i,m}(k)$ as shown below

$$X_{i,m}(k) = \begin{cases} 1, & \text{if } i = m \\ \pm 1, & \text{if } i \neq m. \end{cases} \tag{8}$$

Further, with (7), the correlation term $M_{i,m}(k)M^*_{i,m}(k+1)$ is

$$\begin{aligned} M_{i,m}(k)M^*_{i,m}(k+1) &= H(k)H^*(k+1) \\ &\quad \times X_{i,m}(k)X^*_{i,m}(k+1) \\ &\quad \times (\tfrac{\sin(\pi\epsilon)}{N\sin(\frac{\pi\epsilon}{N})})^2 e^{j\frac{2\pi\tau}{N}} + \bar{W}, \end{aligned} \tag{9}$$

where $M^*_{i,m}(k+1)$ is the complex conjugate of $M_{i,m}(k+1)$ and

$$\begin{aligned} \bar{W} &= H(k)X_{i,m}(k)L(k) \\ &\quad \times [I^*(k+1)P_m(k+1) + W^*(k+1)P_m(k+1)e^{j\frac{2\pi k\tau}{N}}] \\ &\quad + I(k)P_m(k) \times [H^*(k+1)X_{i,m}(k+1)L^*(k+1) \\ &\quad + W^*(k+1)P_m(k+1)e^{j\frac{2\pi k\tau}{N}}] \\ &\quad + W(k)P_m(k)e^{j\frac{-2\pi k\tau}{N}} \\ &\quad \times [H^*(k+1)X_{i,m}(k+1)L^*(k+1) \\ &\quad + I^*(k+1)P_m(k+1)] \\ &\quad + I(k)P_m(k)I^*(k+1)P_m(k+1) \\ &\quad + W(k)P_m(k)W^*(k+1)P_m(k+1) \end{aligned} \tag{10}$$

With (8), by ignoring the noise term $\bar{W}$ and assuming similar frequency responses at the neighbor subcarriers (i.e., $H(k) \approx H(k+1)$), (9) can be reduced to

$$M_{i,m}(k)M^*_{i,m}(k+1) \approx \begin{cases} |H(k)|^2 \times (\frac{\sin(\pi\epsilon)}{N\sin(\frac{\pi\epsilon}{N})})^2 e^{j\frac{2\pi\tau}{N}}, \\ \text{when } i = m \\ \pm|H(k)|^2 \times (\frac{\sin(\pi\epsilon)}{N\sin(\frac{\pi\epsilon}{N})})^2 e^{j\frac{2\pi\tau}{N}}, \\ \text{when } i \neq m \end{cases} \tag{11}$$

where $|(.)|$ is the absolute-value operation.

Basically, with (11), the differential autocorrelation technique of the conventional cell ID detection methods identifies cell preamble index i by detecting the maximum value of the following correlation metric [8][9][10][11] .

$$\hat{i} = \arg \max_{0\leq m\leq M-1} \sum_{k=0}^{N-2} M_{i,m}(k)M^*_{i,m}(k+1). \tag{12}$$

Note that (12) is equivalent to (6).

Since the result of the differential autocorrelation $\sum_{k=0}^{N-2} M_{i,m}(k)M^*_{i,m}(k+1)$ is generally a complex number in practical situations, the maximum-value search process (i.e., $argmax$) should compare the magnitude of the differential autocorrelation. As such, the conventional differential autocorrelation method should be

$$\hat{i} = \arg \max_{0\leq m\leq M-1} |\sum_{k=0}^{N-2} M_{i,m}(k)M^*_{i,m}(k+1)|. \tag{13}$$

Moreover, with the obtaining the magnitude, the effects of the residual frequency offset and the residual timing error can be eliminated as well. However, it would involve high-complexity square-root operations in obtaining the magnitude of the differential autocorrelation. For reducing the complexity, the absolute-value operations can be replaced with the squared absolute-value operations. Each squared absolute-value operation only involves two real-number square operations and a real-number addition operation. Hence, (13) can be adjusted to

$$\hat{i} = \arg \max_{0\leq m\leq M-1} |\sum_{k=0}^{N-2} M_{i,m}(k)M^*_{i,m}(k+1)|^2. \tag{14}$$

For further complexity reduction, this work will simplify the absolute-value operations in (13) by adopting another approach, which will be presented in Section V. Besides, Section V will also compare the conventional methods in all the mentioned forms (i.e., (13), (14), and (45) in Section V) with the proposed methods.

III. Proposed Cell ID Detection Methods

The mentioned conventional cell ID detection methods are subject to noise interference and frequency-selective channel effect (when the assumption of $H(k) \approx H(k+1)$ frequently fails), which lead to performance degradation. In order to enhance the performances of cell ID detection and reduce the complexities, this work proposes the following channel-effect-resilient cell ID detection method (CERCD-I) to mitigate the effects of AWGN and fading channels,

$$\hat{i}_I = \arg \max_{0\leq m\leq M-1} \sum_{k=0}^{N-R} |S_{i,m}(k)|, \tag{15}$$

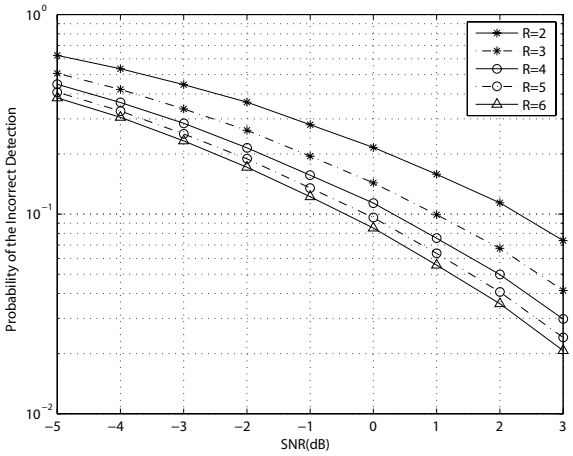

Fig. 2. The probability of the incorrect cell ID detection in a 6-path Rayleigh fading channel of the ITU-R vehicular A channel model.

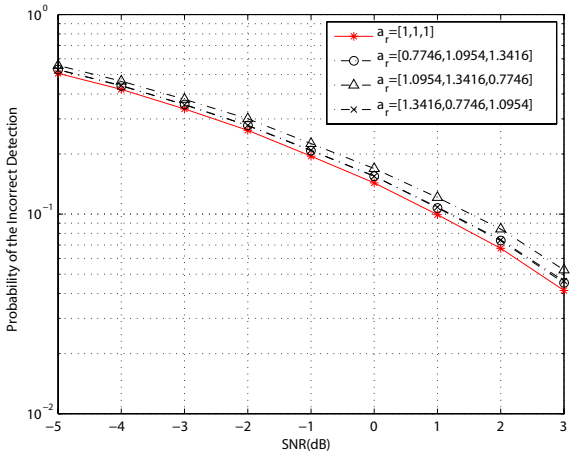

Fig. 3. The probability of the incorrect cell ID detection in a 6-path Rayleigh fading channel of the ITU-R vehicular A channel model.

based on a new optimization metric $S_{i,m}(k)$ defined below

$$S_{i,m}(k) \equiv \sum_{r=0}^{R-1} a_r \times M_{i,m}(k+r), \tag{16}$$

where a_r is the signal smoothing coefficient, and R is the number of the smoothed $M_{i,m}(k)$ terms.

For determining parameter R, one can first consider the features of the optimization metric $S_{i,m}(k)$. Since the proposed method utilizes the concept of the signal filtering in $S_{i,m}(k)$, one can expect that better performance will be achieved by taking more $M_{i,m}(k)$ terms into consideration. As such, as shown in Fig. 2, a higher R leads to a better system performance. However, a lager R corresponds to a higher computational complexity than a smaller R. Besides, the ID detection performance will be decreased, when R is increased to some large value and beyond, even when there is a match in the preamble sequence. It is because that for channels with high frequency response variations, a large enough R will produce a small average gain over the covered R subcarrier channel frequency responses. Therefore, the selection of R is channel dependent and generally a larger R performs better than a smaller R in some limited range of R values. According to our simulation, the performance is proportional to R but saturates at about $R = 5$. However, for the consideration of low-complexity realization, we choose $R = 3$ which provides better performances than conventional methods and achieves low computational complexities in the meantime.

Regarding the weighting parameter a_r on $M_{i,m}(k)$, since we are assuming non-coherent ID detection and dealing with random channels, statistically all the subcarriers are equally important. Therefore, intuitively the performance of optimization metric $S_{i,m}(k)$ with equal a_r weight on each $M_{i,m}(k)$ will outperform the performance of $S_{i,m}(k)$ with unequal a_rs, as verified and shown in Fig. 3. In Fig. 3, different a_r sets are assumed to have the same power for a fair comparison (i.e., $\sum_{r=0}^{R-1} a_r^2$ are the same for all the compared a_r sets). Also a_r should better be some trivial numbers for a low-complexity realization. Therefore, all a_rs are equal to one and it is a good choice for noise smoothing operation. According to the above reasons, we set $R = 3$ and $a_r = 1$ in the discussion for the demonstration of the proposed concept.

As such, the proposed metric $S_{i,m}(k)$ is

$$S_{i,m}(k) = M_{i,m}(k) + M_{i,m}(k+1) + M_{i,m}(k+2). \tag{17}$$

Clearly, in (17), there only needs two complex additions in contrast to the complex multiplication in (11) required by conventional techniques. As will be shown later, by applying this metric to determine the cell ID, much higher performance and lower computational complexity can be achieved compared with conventional techniques.

Next, we will briefly discuss the concept of the proposed metric. By substituting (7) into (17), $S_{i,m}(k)$ can be rewritten as

$$\begin{aligned} S_{i,m}(k) &= H(k)X_{i,m}(k)L(k) \\ &\quad + H(k+1)X_{i,m}(k+1)L(k+1) \\ &\quad + H(k+2)X_{i,m}(k+2)L(k+2) + e_I + e_w, \end{aligned} \tag{18}$$

where

$$e_I \equiv I(k)P_m(k) + I(k+1)P_m(k+1) + I(k+2)P_m(k+2)$$

and

$$\begin{aligned} e_w \quad &\equiv W(k)P_m(k)e^{j\frac{-2\pi k\tau}{N}} \\ &\quad + W(k+1)P_m(k+1)e^{j\frac{-2\pi(k+1)\tau}{N}} \\ &\quad + W(k+2)P_m(k+2)e^{j\frac{-2\pi(k+2)\tau}{N}}. \end{aligned}$$

Note that $H(k)$ and $W(k)$ terms are approximately assumed complex Gaussian random variables. Moreover, by substitut-

ing $I(k)$ into e_I, the e_I can be further expressed as

$$\begin{aligned} e_I \quad &\equiv I(k)P_m(k) + I(k+1)P_m(k+1) \\ &\quad + I(k+2)P_m(k+2) \\ &= \textstyle\sum_{m=0,m\neq k}^{N-1} H(m)P_i(m)P_m(k) \\ &\quad \times \frac{\sin(\pi(\epsilon+k-m))}{N\sin(\frac{\pi(\epsilon+k-m)}{N})} e^{j\frac{\pi(\epsilon+k-m)(N-1)}{N}} e^{j\frac{-2\pi k\tau}{N}} \\ &\quad + \textstyle\sum_{m=0,m\neq k+1}^{N-1} H(m)P_i(m)P_m(k+1) \\ &\quad \times \frac{\sin(\pi(\epsilon+k+1-m))}{N\sin(\frac{\pi(\epsilon+k+1-m)}{N})} e^{j\frac{\pi(\epsilon+k+1-m)(N-1)}{N}} e^{j\frac{-2\pi(k+1)\tau}{N}} \\ &\quad + \textstyle\sum_{m=0,m\neq k+2}^{N-1} H(m)P_i(m)P_m(k+2) \\ &\quad \times \frac{\sin(\pi(\epsilon+k+2-m))}{N\sin(\frac{\pi(\epsilon+k+2-m)}{N})} e^{j\frac{\pi(\epsilon+k+2-m)(N-1)}{N}} e^{j\frac{-2\pi(k+2)\tau}{N}} \end{aligned} \tag{19}$$

According to (19), $P_i(m)P_m(k)$, $P_i(m)P_m(k+1)$, and $P_i(m)P_m(k+2)$ lead to the randomness of e_I.

With (18), $|S_{i,m}(k)|$ can be further expanded as

$$|S_{i,m}(k)| = \sqrt{A(k) + B_{i,m}(k) + C_{i,m}(k) + D_{i,m}(k)}, \tag{20}$$

where

$$A(k) \equiv \left(\frac{\sin(\pi\epsilon)}{N\sin(\frac{\pi\epsilon}{N})}\right)^2 \times \left(|H(k)|^2 + |H(k+1)|^2 + |H(k+2)|^2\right),$$

$$\begin{aligned} B_{i,m}(k) \equiv\ & H(k)X_{i,m}(k)L(k)e_w^* \\ & + H(k+1)X_{i,m}(k+1)L(k+1)e_w^* \\ & + H(k+2)X_{i,m}(k+2)L(k+2)e_w^* \\ & + H^*(k)X_{i,m}^*(k)L^*(k)e_w \\ & + H^*(k+1)X_{i,m}^*(k+1)L^*(k+1)e_w \\ & + H^*(k+2)X_{i,m}^*(k+2)L^*(k+2)e_w \\ & + e_I e_w^* + e_I^* e_w + |e_w|^2, \end{aligned}$$

$$\begin{aligned} C_{i,m}(k) \equiv\ & H(k)X_{i,m}(k)L(k)e_I^* \\ & + H(k+1)X_{i,m}(k+1)L(k+1)e_I^* \\ & + H(k+2)X_{i,m}(k+2)L(k+2)e_I^* \\ & + H^*(k)X_{i,m}^*(k)L^*(k)e_I \\ & + H^*(k+1)X_{i,m}^*(k+1)L^*(k+1)e_I \\ & + H^*(k+2)X_{i,m}^*(k+2)L^*(k+2)e_I \\ & + |e_I|^2, \end{aligned}$$

and

$$\begin{aligned} D_{i,m}(k) \equiv\ & I_{i,m1}(k) \times \left(\frac{\sin(\pi\epsilon)}{N\sin(\frac{\pi\epsilon}{N})}\right)^2 \\ & \times [H(k)H^*(k+1)e^{j\frac{2\pi\tau}{N}} + H^*(k)H(k+1)e^{j\frac{-2\pi\tau}{N}}] \\ & + I_{i,m2}(k) \times \left(\frac{\sin(\pi\epsilon)}{N\sin(\frac{\pi\epsilon}{N})}\right)^2 \\ & \times [H(k)H^*(k+2)e^{j\frac{4\pi\tau}{N}} + H^*(k)H(k+2)e^{j\frac{-4\pi\tau}{N}}] \\ & + I_{i,m3}(k) \times \left(\frac{\sin(\pi\epsilon)}{N\sin(\frac{\pi\epsilon}{N})}\right)^2 \\ & \times [H(k+1)H^*(k+2)e^{j\frac{2\pi\tau}{N}} \\ & \quad + H^*(k+1)H(k+2)e^{j\frac{-2\pi\tau}{N}}], \end{aligned}$$

and

$$\begin{cases} I_{i,m1}(k) \equiv X_{i,m}(k)X_{i,m}(k+1) \\ I_{i,m2}(k) \equiv X_{i,m}(k)X_{i,m}(k+2) \\ I_{i,m3}(k) \equiv X_{i,m}(k+1)X_{i,m}(k+2). \end{cases}$$

As shown, $|S_{i,m}(k)|$ consists of four parts. The first part, $A(k)$, contains the channel power terms and the second part, $B_{i,m}(k)$, contains the multiplication terms of AWGN, channel responses and preamble signals. Then, $C_{i,m}(k)$ contains the multiplication terms of ICI, channel responses and preamble signals. Finally, the fourth part, $D_{i,m}(k)$, consists of multiplication terms of the preamble signals and subcarrier responses.

Note that $A(k)$ is independent of the preamble index m. On the other hand, $B_{i,m}(k)$ and $C_{i,m}(k)$ corresponds to noise smoothing and lowpass filtering operations which lead to significantly attenuated results, due to the randomness of $B_{i,m}(k)$ and $C_{i,m}(k)$ caused by the AWGN components and e_I, respectively. Hence, $B_{i,m}(k)$ and $C_{i,m}(k)$ are generally small and insignificant in (20) for all m values. Finally, $D_{i,m}(k)$ plays the most dominant role in (20), because the $I_{i,m}(k)$ terms represent the preamble matching values of $X_{i,m}(k)$, $X_{i,m}(k+1)$ and $X_{i,m}(k+2)$. If $m = i$, the accumulated $|S_{i,m}(k)|$ will statistically generate a maximum value among all the possible m values. Thus, with (15), the cell ID with the maximum accumulated magnitude of the proposed metrics, among all the accumulated magnitudes, will be the detected.

Further, it should be also noted that the proposed methods can be generalized to flexibly detect the cell ID by dividing the input into either overlapping or non-overlapping summation segments, subject to cost-and-performance tradeoff. As such, the proposed methods can be generalized to include the method in [21]. The code group identification method in [21] can be derived from the proposed CERCD-I method by setting the parameters of CERCD-I to $R = 64$ and $a_r = 1$ and adjusting the values of accumulation index k to $k = \{0,\ 64,\ 128,\ 192\}$. Since the amount (i.e., 193, $k = \{0, 1, ..., 192\}$) of accumulated $|S_{i,m}(k)|$ terms for the CERCD-I method is much larger than that (i.e., 4, $k = \{0,\ 64,\ 128,\ 192\}$) for the method in [21], performance of the proposed method will be better than the method in [21], in terms of robustness to fading channels . Regarding complexity comparison, owing to the difference in the accumulation terms, the method in [21] has a lower complexity than the CERCD-I method.

However, the proposed CERCD-I method (15) still requires high-complexity square-root operations. Since intuitively $|S_{i,m}(k)|^2$ has similar behavior to $|S_{i,m}(k)|$, the second proposed cell ID detection method (CERCD-II) simply replaces the high-complexity absolute-value operations with the squared absolute-value operations as follows,

$$\hat{i}_{II} = \arg\max_{0\leq m\leq M-1} \textstyle\sum_{k=0}^{N-3} |S_{i,m}(k)|^2. \tag{21}$$

Moreover, with (20), both CERCD-I and CERCD-II methods can be rewritten as

$$\begin{aligned} \hat{i}_I = \arg\max_{0\leq m\leq M-1} \quad & \textstyle\sum_{k=0}^{N-3} \{A(k) + B_{i,m}(k) \\ & + C_{i,m}(k) + D_{i,m}(k)\}^{\frac{1}{2}} \end{aligned} \tag{22}$$

and

$$\hat{i}_{II} = \arg\max_{0\le m\le M-1} \quad \sum_{k=0}^{N-3}\{A(k)+B_{i,m}(k) + C_{i,m}(k)+D_{i,m}(k)\}, \tag{23}$$

respectively. In CERCD-I method, since the noise term $B_{i,m}(k)$ and $C_{i,m}(k)$ in (22) are inside their respective magnitude of $S_{i,m}(k)$ (i.e., inside the square-root operation), all the $B_{i,m}(k)$ and $C_{i,m}(k)$ terms will not be averaged out in the accumulation operations. By contrast, in CERCD-II method, all the $B_{i,m}(k)$ and $C_{i,m}(k)$ terms in (23) are accumulated directly. Consequently, the noise terms $B_{i,m}(k)$ and $C_{i,m}(k)$ will be smoothed and reduced. As a result, CERCD-II method is expected to have better performance than CERCD-I method as will be verified by simulations later.

Further, the complexity of CERCD-I method can be significantly reduced by approximating the absolute-value operations in (15) with

$$|S_{i,m}(k)| \approx |Re\{S_{i,m}(k)\}| + |Im\{S_{i,m}(k)\}|. \tag{24}$$

For the convenience of ensuing discussion, let the approximation be defined as

$$\| S_{i,m}(k) \| \equiv |Re\{S_{i,m}(k)\}| + |Im\{S_{i,m}(k)\}|. \tag{25}$$

As will be demonstrated later, in the maximum-value search process (i.e., $argmax$), this approximation will introduce slight performance impairment, but with much reduced complexity. Therefore, by applying (25) to (15), this work proposes the following third cell ID detection method (named CERCD-III method).

$$\hat{i}_{III} = \arg \max_{0\le m\le M-1} \sum_{k=0}^{N-3} \| S_{i,m}(k) \|. \tag{26}$$

As will be shown later, by applying the new optimization metric to smooth the channel variation and AWGN, all the proposed methods will have better performances than the conventional methods conceptually. Moreover, it will be shown that the performance of CERCD-III method is very close to that of CERCD-I method but with the least complexity among all the proposed methods. Hence, CERCD-III method is more suitable for realization than CERCD-I and CERCD-II methods. Next, we will provide the theoretical analysis of CERCD-III method, followed by the performance and complexity comparisons between the conventional and proposed methods.

IV. Theoretical Analysis

Since the proposed CERCD-III method is preferred for realization, this section will derive its statistical properties which include the mean performance and the variance's lower bound. Without loss of generality and for the consideration of simplicity and readability, the derivation is performed assuming a two-path Rayleigh-fading channel. Note that the derived result can be easily extended to the conditions of more than two paths.

First of all, for convenience, let us define

$$\begin{aligned} F_{i,m} &\equiv \sum_{k=0}^{N-3} \| S_{i,m}(k) \| \\ &= \sum_{k=0}^{N-3} (|Re\{S_{i,m}(k)\}| + |Im\{S_{i,m}(k)\}|). \end{aligned} \tag{27}$$

Since both $Re\{S_{i,m}(k)\}$ and $Im\{S_{i,m}(k)\}$ have the same distribution and statistical values, it is sufficient to only analyze $Re\{S_{i,m}(k)\}$.

Moreover, for obtaining the distribution of the proposed estimates, the whole analysis can be separated into four parts. The first part discusses the relationships of statistical values (i.e., mean and variance) between $Re\{S_{i,m}(k)\}$ and $|Re\{S_{i,m}(k)\}|$. Then, based on the result, the second part obtains the statistical values of $\| S_{i,m}(k) \|$ in terms of the statistical values of $Re\{S_{i,m}(k)\}$ and $Im\{S_{i,m}(k)\}$. The third part investigates the variance of $Re\{S_{i,m}(k)\}$. Finally, the distribution of $F_{i,m}$ will be derived in the last part.

Since a two-path fading channel is assumed, the channel response is

$$\begin{aligned} H(k) &= \sum_{l=0}^{L-1} h_l e^{\frac{-j2\pi lk}{N}} \\ &= h_{l_0} e^{\frac{-j2\pi l_0 k}{N}} + h_{L-1} e^{\frac{-j2\pi (L-1)k}{N}}. \end{aligned} \tag{28}$$

where h_l is the l-th channel path. Note that l_0 is a positive integer and $0 \le l_0 \le L-1$; $h_l = 0$, for $l \ne l_0$ and $l \ne L-1$. For notational simplicity, let us define $\bar{H}_{l_0}(k) \equiv h_{l_0} e^{\frac{-j2\pi l_0 k}{N}}$ and $\bar{H}_{L-1}(k) \equiv h_{L-1} e^{\frac{-j2\pi (L-1)k}{N}}$. Hence, by substituting (28) into (18), (18) can be rewritten as

$$S_{i,m}(k) = \bar{H}_{l_0}(k)\bar{X}_{i,m,l_0}(k) + \bar{H}_{L-1}(k)\bar{X}_{i,m,L-1}(k) + e_I + e_w, \tag{29}$$

where

$$\begin{aligned} \bar{X}_{i,m,l}(k) &= \frac{\sin(\pi\epsilon)}{N\sin(\frac{\pi\epsilon}{N})} e^{j\frac{\pi(N\epsilon-\epsilon-2k\tau)}{N}} \\ &\quad \times \{X_{i,m}(k) + X_{i,m}(k+1)e^{\frac{-j2\pi(l+\tau)}{N}} \\ &\quad + X_{i,m}(k+2)e^{\frac{-j4\pi(l+\tau)}{N}}\}. \end{aligned}$$

Moreover, according to (8), one can obtain the following mean values of $E\{\bar{X}_{i,m,l_0}(k)^2\}$ and $E\{\bar{X}_{i,m,L-1}(k)^2\}$.

$$E\{\bar{X}_{i,m,l_0}(k)^2\} = E\{\bar{X}_{i,m,L-1}(k)^2\} = \begin{cases} 9 \times (\frac{\sin(\pi\epsilon)}{N\sin(\frac{\pi\epsilon}{N})})^2, \\ \text{if } i = m \\ \\ 3 \times (\frac{\sin(\pi\epsilon)}{N\sin(\frac{\pi\epsilon}{N})})^2, \\ \text{if } i \ne m. \end{cases} \tag{30}$$

Moreover, in the theoretical analysis, the mean and the variance of a general random variable X are defined as μ_X and σ_X^2, respectively.

A. Statistical Relationship Between $Re\{S_{i,m}(k)\}$ and $|Re\{S_{i,m}(k)\}|$

As described in Section III, since all the components inside $S_{i,m}(k)$ are assumed complex Gaussian distribution, $S_{i,m}(k)$ is approximately a complex Gaussian random variable with zero mean. As a result, the probability density function

(PDF) of $|Re\{S_{i,m}(k)\}|$ is a folded normal distribution [16]. Hence, the statistical values (including mean and variance) of $Re\{S_{i,m}(k)\}$ and $|Re\{S_{i,m}(k)\}|$ can be further shown [16] to be related by

$$\begin{cases} \mu_{|Re\{S_{i,m}(k)\}|} \\ = \sigma_{Re\{S_{i,m}(k)\}}\sqrt{\frac{2}{\pi}}exp(\frac{-\mu^2_{Re\{S_{i,m}(k)\}}}{2\sigma^2_{Re\{S_{i,m}(k)\}}}) \\ +\mu_{Re\{S_{i,m}(k)\}}[1-2\Phi(\frac{-\mu_{Re\{S_{i,m}(k)\}}}{\sigma_{Re\{S_{i,m}(k)\}}})] \\ \\ \sigma^2_{|Re\{S_{i,m}(k)\}|} \\ = \mu^2_{Re\{S_{i,m}(k)\}} + \sigma^2_{Re\{S_{i,m}(k)\}} - \mu^2_{|Re\{S_{i,m}(k)\}|}, \end{cases} \quad (31)$$

where $\Phi(.)$ denotes the cumulative distribution function (CDF) of a standard normal distribution. Similarly, $|Im\{S_{i,m}(k)\}|$ is also a random variable with folded normal distribution. Moreover, $Im\{S_{i,m}(k)\}$ and $|Im\{S_{i,m}(k)\}|$ have the same relationship as (31).

B. The Statistical Values of $\| S_{i,m}(k) \|$

With (25), (31) and $\mu_{S_{i,m}(k)} = 0$, the mean and the variance of $\| S_{i,m}(k) \|$ become

$$\mu_{\|S_{i,m}(k)\|} = \sqrt{\frac{2}{\pi}}(\sigma_{Re\{S_{i,m}(k)\}} + \sigma_{Im\{S_{i,m}(k)\}}) \quad (32)$$

and

$$\sigma^2_{\|S_{i,m}(k)\|} = (1-\frac{2}{\pi})(\sigma^2_{Re\{S_{i,m}(k)\}} + \sigma^2_{Im\{S_{i,m}(k)\}}), \quad (33)$$

respectively. Next, the values of $\sigma_{Re\{S_{i,m}(k)\}}$ and $\sigma_{Im\{S_{i,m}(k)\}}$ in (32) and (33) are derived as follows.

C. Derivation of $\sigma^2_{Re\{S_{i,m}(k)\}}$

With (29), $\sigma^2_{Re\{S_{i,m}(k)\}}$ can be represented as

$$\begin{aligned} \sigma^2_{Re\{S_{i,m}(k)\}} &= \sigma^2_{Re\{\bar{H}_{l_0}(k)\bar{X}_{i,m,l_0}(k)\}} \\ &+\sigma^2_{Re\{\bar{H}_{L-1}(k)\bar{X}_{i,m,L-1}(k)\}} \\ &+\sigma^2_{Re\{e_w\}}, \end{aligned} \quad (34)$$

Further, with $\mu_{Re\{S_{i,m}(k)\}} = 0$ and the independence between $\bar{H}_l(k)$ and $\bar{X}_{i,m,l}(k)$, (34) can be rewritten as

$$\begin{aligned} \sigma^2_{Re\{S_{i,m}(k)\}} &= E\{\bar{X}_{i,m,l_0}(k)^2\}E\{Re^2\{\bar{H}_{l_0}(k)\}\} \\ &+E\{\bar{X}_{i,m,L-1}(k)^2\}E\{Re^2\{\bar{H}_{L-1}(k)\}\} \\ &+E\{Re^2\{W(k)\}\} + E\{Re^2\{W(k+1)\}\} \\ &+E\{Re^2\{W(k+2)\}\}. \end{aligned} \quad (35)$$

For obtaining each $E\{Re^2\{.\}\}$ term in (35) such as $E\{Re^2\{\bar{H}_{l_0}(k)\}\}$, $E\{Re^2\{\bar{H}_{L-1}(k)\}\}$, and etc., one can use the following property. If random variable X is a Gaussian distribution, namely, $X \sim N(\mu_X, \sigma^2_X)$, then $(\frac{X}{\sigma_X})^2$ will be a noncentral chi-square distribution whose degree of freedom is one and the noncentrality parameter is $\lambda = (\frac{\mu_X}{\sigma_X})^2$. Consequently, the mean and variance of X^2 are given by $\mu_{X^2} = \mu^2_X + \sigma^2_X$ and $\sigma^2_{X^2} = 2\sigma^4_X + 4\mu^2_X\sigma^2_X$, respectively. In (35), based on the fact that each random variable in $Re\{.\}$ is a Gaussian distribution with zero mean, one can derive the following terms by applying the mentioned property.

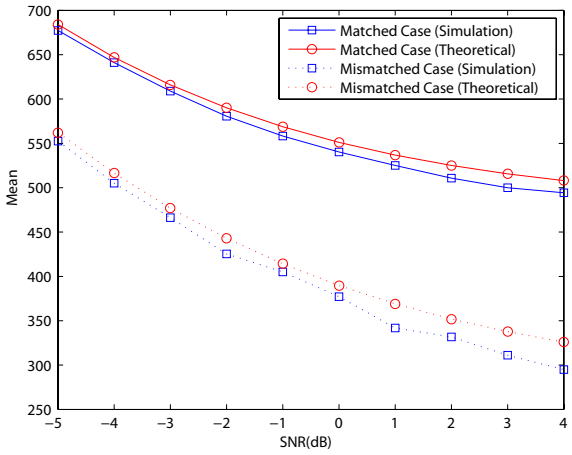

Fig. 4. The means of $F_{i,m}$ in a multipath Rayleigh fading channel with two equal-power paths when $N = 512$, $\epsilon = 0$, and $\tau = 4$.

$$\begin{cases} E\{Re^2\{\bar{H}_{l_0}(k)\}\} = \frac{\sigma^2_{h_{l_0}}}{2} \\ E\{Re^2\{\bar{H}_{L-1}(k)\}\} = \frac{\sigma^2_{h_{L-1}}}{2} \\ E\{Re^2\{W(k)\}\} = \frac{\sigma^2_w}{2} \\ E\{Re^2\{W(k+1)\}\} = \frac{\sigma^2_w}{2} \\ E\{Re^2\{W(k+2)\}\} = \frac{\sigma^2_w}{2}. \end{cases} \quad (36)$$

Therefore, after substituting (30) and (36) into (35) directly, (35) can be reduced to

$$\sigma^2_{Re\{S_{i,m}(k)\}} = \begin{cases} \frac{9}{2}\times(\frac{\sin(\pi\epsilon)}{N\sin(\frac{\pi\epsilon}{N})})^2\times\sigma^2_{h_{l_0}} \\ +\frac{9}{2}\times(\frac{\sin(\pi\epsilon)}{N\sin(\frac{\pi\epsilon}{N})})^2\times\sigma^2_{h_{L-1}} + \frac{3}{2}\sigma^2_w, \\ \text{if } i = m \\ \\ \frac{3}{2}\times(\frac{\sin(\pi\epsilon)}{N\sin(\frac{\pi\epsilon}{N})})^2\times\sigma^2_{h_{l_0}} \\ +\frac{3}{2}\times(\frac{\sin(\pi\epsilon)}{N\sin(\frac{\pi\epsilon}{N})})^2\times\sigma^2_{h_{L-1}} + \frac{3}{2}\sigma^2_w, \\ \text{if } i \neq m. \end{cases} \quad (37)$$

Similarly, the variance of $Im\{S_{i,m}(k)\}$, $\sigma^2_{Im\{S_{i,m}(k)\}}$, can be obtained through the same derivation.

D. The distribution of $F_{i,m}$

With the definition of $F_{i,m}$ in (27), by substituting (37) into (32) and (33), the mean and variance of $F_{i,m}$ are

$$\mu_{F_{i,m}} = \sum_{k=0}^{N-3}\mu_{\|S_{i,m}(k)\|} \quad (38)$$

and

$$\begin{aligned} \sigma^2_{F_{i,m}} &= \sum_{k=0}^{N-3}\sigma^2_{\|S_{i,m}(k)\|} \\ &+ 2\times\sum_{k_1,k_2=0;k_1<k_2}^{N-3}\rho_{i,m}(k_1,k_2)\sigma_{\|S_{i,m}(k_1)\|}\sigma_{\|S_{i,m}(k_2)\|}, \end{aligned} \quad (39)$$

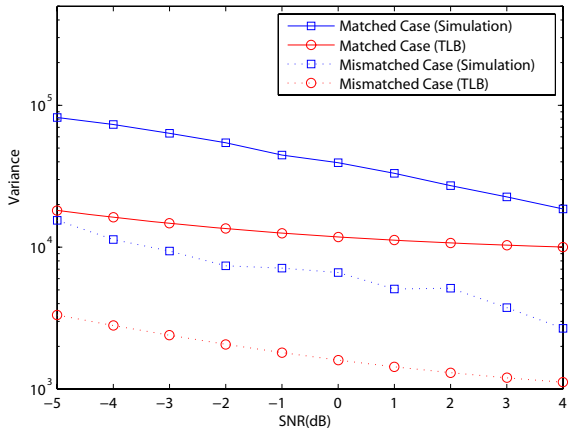

Fig. 5. The variances of $F_{i,m}$ in a multipath Rayleigh fading channel with two equal-power paths when $N = 512$, $\epsilon = 0$, and $\tau = 4$.

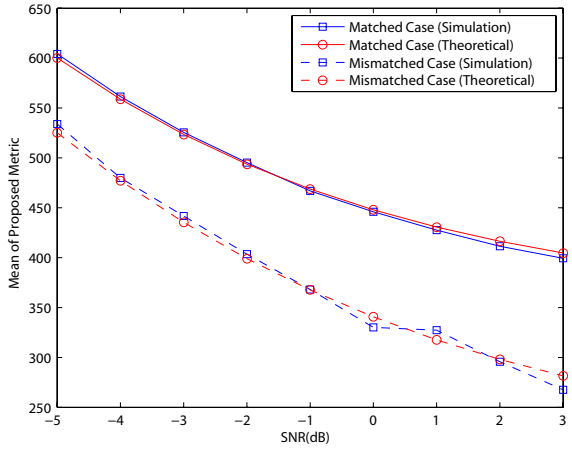

Fig. 6. The means of $F_{i,m}$ in a multipath Rayleigh fading channel with two equal-power paths when $N = 512$, $\epsilon = 0.4$, and $\tau = 4$.

respectively, where $\rho_{i,m}(k_1, k_2)$ is the correlation coefficient between $\| S_{i,m}(k_1) \|$ and $\| S_{i,m}(k_2) \|$. Since $\sigma_{\|S_{i,m}(k)\|}$ is the same for all subcarriers, $\sigma^2_{F_{i,m}}$ can be further reduced to

$$\sigma^2_{F_{i,m}} = \sum_{k=0}^{N-3} \sigma^2_{\|S_{i,m}(k)\|} + 2\sigma^2_{\|S_{i,m}(k)\|} \times \sum_{k_1,k_2=0;k_1<k_2}^{N-3} \rho_{i,m}(k_1, k_2), \quad (40)$$

For the simplification of the second component in (40), we assume a common correlation coefficient $\bar{\rho}_{i,m}$ instead of determining each distinct $\rho_{i,m}(k_1, k_2)$. Since there are correlatedness between the adjacent subcarriers, each distinct $\rho_{i,m}(k_1, k_2)$ will be higher than the common correlation coefficient. That is, $\sum_{k_1,k_2=0;k_1<k_2}^{N-3} \rho_{i,m}(k_1, k_2)$ will be higher than $\frac{(N-2)(N-3)\bar{\rho}_{i,m}}{2}$. Hence, the following variance derivation represents the lower bound of the proposed method and (40) can be rewritten as

$$\sigma^2_{F_{i,m}} \geq \sum_{k=0}^{N-3} \sigma^2_{\|S_{i,m}(k)\|} + (N-2)(N-3)\sigma^2_{\|S_{i,m}(k)\|}\bar{\rho}_{i,m}. \quad (41)$$

By applying the method of Pearson product-moment correlation coefficient [18] and from simulation, the common correlation coefficients, $\bar{\rho}_{i,m}$, can be approximated as

$$\bar{\rho}_{i,m} \approx \begin{cases} 0.13, & \text{if } i = m \\ 0.03, & \text{if } i \neq m. \end{cases} \quad (42)$$

Finally, by substituting (32) and (37) into (38), one can obtain the following mean of $F_{i,m}$

$$\mu_{F_{i,m}} = \begin{cases} (N-2) \times \left(\frac{(36\sigma^2_{h_0}+36\sigma^2_{h_{L-1}})\times(\frac{\sin(\pi\epsilon)}{N\sin(\frac{\pi\epsilon}{N})})^2+12\sigma^2_w}{\pi}\right)^{\frac{1}{2}}, \\ \text{if } i = m \\ (N-2) \times \left(\frac{(12\sigma^2_{h_0}+12\sigma^2_{h_{L-1}})\times(\frac{\sin(\pi\epsilon)}{N\sin(\frac{\pi\epsilon}{N})})^2+12\sigma^2_w}{\pi}\right)^{\frac{1}{2}}, \\ \text{if } i \neq m. \end{cases} \quad (43)$$

On the other hand, by substituting (33) and (37) into (41), the lower bound of the variance of $F_{i,m}$ can be shown to be

$$\sigma^2_{F_{i,m}} \geq \begin{cases} (N^2\bar{\rho}_{i,m} - 5N\bar{\rho}_{i,m} + 6\bar{\rho}_{i,m} + N - 2) \times (1 - \frac{2}{\pi}) \\ \times\{(9\sigma^2_{h_0} + 9\sigma^2_{h_{L-1}}) \times (\frac{\sin(\pi\epsilon)}{N\sin(\frac{\pi\epsilon}{N})})^2 + 3\sigma^2_w\}, \\ \text{if } i = m \\ (N^2\bar{\rho}_{i,m} - 5N\bar{\rho}_{i,m} + 6\bar{\rho}_{i,m} + N - 2) \times (1 - \frac{2}{\pi}) \\ \times\{(3\sigma^2_{h_0} + 3\sigma^2_{h_{L-1}}) \times (\frac{\sin(\pi\epsilon)}{N\sin(\frac{\pi\epsilon}{N})})^2 + 3\sigma^2_w\}, \\ \text{if } i \neq m. \end{cases} \quad (44)$$

Although the above theoretical analysis focuses on the case with $R = 3$ and $a_r = 1$, it still can provide some ideas about the performances under different Rs and a_rs intuitively. Since (30) depends on R, a larger R will result in a larger difference between the results of $i = m$ and $i \neq m$ in (30) than the case with a smaller R. For examples, when $R = 4$, the results of $i = m$ and $i \neq m$ in (30) will become $16 \times (\frac{\sin(\pi\epsilon)}{N\sin(\frac{\pi\epsilon}{N})})^2$ and $4 \times (\frac{\sin(\pi\epsilon)}{N\sin(\frac{\pi\epsilon}{N})})^2$, respectively. Clearly, in this case, the

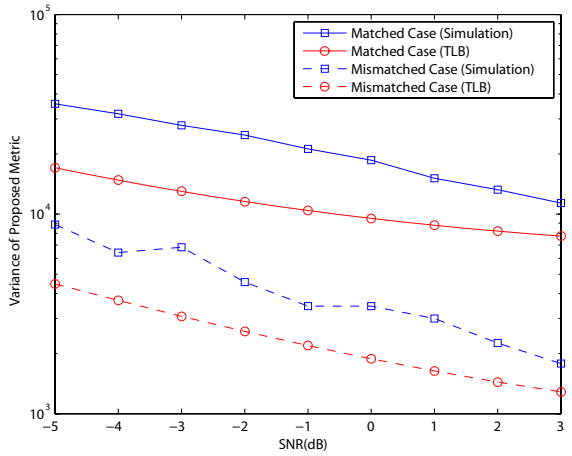

Fig. 7. The variances of $F_{i,m}$ in a multipath Rayleigh fading channel with two equal-power paths when $N = 512$, $\epsilon = 0.4$, and $\tau = 4$.

TABLE I
COMPLEXITIES OF THE PROPOSED METHODS AND COMPLEXITY COMPARISON

Techniques	No. of Real-number Multiplication Operations	No. of Real-number Addition Operations	No. of Absolute-value Operations
Differential Autocorrelation Method (13)	$4M \times (N-2) + 4M$	$4M \times (N-2) + 2M$	M
Differential Autocorrelation Method (14)	$4M \times (N-2) + 8M$	$4M \times (N-2) + 4M$	0
Differential Autocorrelation Method (45)	$4M \times (N-2) + 4M$	$4M \times (N-2) + 3M$	0
Proposed CERCD-I method	0	$5M \times (N-3) + 4M$	$M \times (N-3) + M$
Proposed CERCD-II method	$4M \times (N-3) + 4M$	$7M \times (N-3) + 6M$	0
Proposed CERCD-III method	0	$6M \times (N-3) + 5M$	0

difference between $i = m$ and $i \neq m$ is larger than the case with $R = 3$. Obviously, a larger difference will achieve a better performance than a smaller one. Besides, same a_r on all $M_{i,m}(k)$s is a reasonable choice so that the contributions from all the $X_{i,m}(k)$ terms to $\bar{X}_{i,m,l}(k)$ can be equally considered.

Fig. 4 shows the theoretically derived mean and the simulated mean of $F_{i,m}$, while Fig. 5 shows the simulated variance curves of $F_{i,m}$ due to the matched and mismatched cases, and the theoretical lower bound (TLB) of the variance. Moreover, Fig. 6 and Fig. 7 show similar results under the residual frequency offset $\epsilon = 0.4$ in contrast to the residual frequency offset $\epsilon = 0$ as in Fig. 4 and Fig. 5. In the figures, the matched case means $i = m$, while the mismatched case means $i \neq m$. As observed, regardless of the matched or mismatched cases, the curves of theoretically derived means are very close to the simulation means, while the simulated variances are bounded by the TLBs.

Moreover, by comparing Fig. 4 with Fig. 6, the difference between the means of the matched and the mismatched cases is smaller when there is a higher residual frequency offset in the system. Next, for evaluating the proposed methods, the comparisons of the complexity and the performance between the proposed techniques and the differential autocorrelation techniques will be discussed in the following two sections.

E. Probability of the Incorrect Cell ID Detection

For the probability of the incorrect cell ID detection, it is reasonable to treat the problem of finding the correct cell ID as a hypothesis testing problem. As such, the probability of the incorrect cell ID detection is

$$P_{Inc} = 1 - \prod_{m=0, m\neq i}^{M-1} Pr\{F_{i,m} \leq F_{i,i}\}$$

Note that each $||S_{i,m}(k)||$ in $F_{i,m}$ is a random variable with folded normal distribution. However, the adjacent $||S_{i,m}(k)||$s (i.e., $||S_{i,m}(k)||$, $||S_{i,m}(k+1)||$, ..., and $||S_{i,m}(k+R-1)||$) are not independent, because all of those terms partly contain the same $M_{i,m}(k)$ terms. Thus, one cannot utilize the central limit theorem (CLT) to model $F_{i,m}$ (which is a linear combination of $||S_{i,m}(k)||$) as a Gaussian random variable. As such, it is not that easy and direct to obtain the probability density function (PDF) of $F_{i,m}$, that is, the exact theoretical probability of the incorrect detection. Nevertheless, the discussion about the mean and variance still can exhibit the characteristics of the proposed methods. Especially, if one tries to practically realize the proposed methods with fixed-point operations, those analyses can provide some guidelines about the word-length decision in the implementation.

V. COMPUTATIONAL COMPLEXITY ANALYSIS

First of all, for a fair discussion, similar to the proposed CERCD-III method, the conventional differential autocorrelation technique in (13) can be also simplified as

$$\begin{aligned} \hat{i} &= \arg\max_{0\leq m\leq M-1} \parallel \sum_{k=0}^{N-2} M_{i,m}(k) M_{i,m}^{*}(k) \parallel \\ &= \arg\max_{0\leq m\leq M-1} (|Re\{\sum_{k=0}^{N-2} M_{i,m}(k) M_{i,m}^{*}(k)\} \\ &\qquad + |Im\{\sum_{k=0}^{N-2} M_{i,m}(k) M_{i,m}^{*}(k)\}) \end{aligned} \tag{45}$$

Table I shows the complexity comparison of the conventional and proposed methods. Note that the complexity of each matching operation in (7) is negligible, because the preambles are assumed BPSK-modulated and each matching operation is equivalent to an exclusive-or (XOR) operation of sign bits. The conventional schemes need one complex multiplication in computing $M_{i,m}(k)M_{i,m}^{*}(k+1)$, while all the proposed methods only require two complex additions in calculating $S_{i,m}(k)$.

Moreover, the original form of the conventional methods (i.e., (13)) requires M absolute-value operations and each $|(.)|^2$ operation requires two real-number square operations and a real-number addition operation, while (45) requires a real-number addition operation to perform each $\parallel (.) \parallel$ operation. As for the proposed methods, each $|S_{i,m}(k)|$ in CERCD-I method costs four real-number addition operations and an absolute-value operation, while CERCD-II method requires two real-number multiplication operations and five real-number addition operations for each $|S_{i,m}(k)|^2$. Finally, each $\parallel S_{i,m}(k) \parallel$ in CERCD-III method is realized by five real-number addition operations.

As shown in Table I, the number of multiplication operations of the proposed CERCD-II method is less than the conventional methods of (14) and (45), while the number of additions of the proposed CERCD-II method is more than that of the conventional methods. However, by applying the approximation of (24) to the new metric, the proposed CERCD-III method does not require any multiplication operation. Hence, the proposed CERCD-III method has much lower complexity than all the other methods.

VI. Simulation Results

As mentioned in the introduction, since the current OFDM cell ID methods are all mainly based on the differential autocorrelation technique, the simulations results apply to all the discussed conventional non-coherent methods. For a rigorous assessment of the proposed and the conventional differential autocorrelation techniques, simulation results in different channel conditions are provided. Here, the system simulation parameters are defined as:

- Operating Frequency: 2.5 GHz
- Signal Bandwidth: 5 MHz
- FFT Length: 512
- Cyclic Prefix Length: 128
- Residual Timing Offset (τ): 4 samples
- Residual Frequency Offsets (ϵ): 0 or 0.4
- Normalized Doppler Frequency: 0.1

where the normalized Doppler frequency is equal to the maximum Doppler frequency normalized by the subcarrier spacing.

The simulation channel is based on Jake's Rayleigh fading channel model [17]. The adopted power delay profiles with six paths follow the vehicular test environments of ITU-R model [15] as follows.

- **Vehicular A channel** (Power(dB)/Delay(ns)): 0dB/0ns, $-$1dB/310ns, $-$9dB/710ns, $-$10dB/1090ns, $-$15dB/1730ns, $-$20dB/2510ns
- **Vehicular B channel** (Power(dB)/Delay(ns)): $-$2.5dB/0ns, 0dB/300ns, $-$12.8dB/8900ns, $-$10dB/12900ns, $-$25.2dB/17100ns, $-$16dB/20000ns,

According to power delay profile, the r.m.s. delay spreads of the vehicular A channel and the vehicular B channel are $370.39ns$ and $4001.4ns$, respectively. Furthermore, the coherent bandwidth of A channel and B channel are approximately 539.97kHz and 49.98kHz, respectively. Since those two bandwidths are all narrower than the signal bandwidth, both channels are frequency-selective fading channels. Moreover, channel B is more frequency-selective than channel A, because its coherent bandwidth is narrower than that of A channel.

As shown in Fig. 8, the CERCD-I method with overlapping segments (corresponding to "Overlapping" in the legend of the figure) have better performances than the code group identification methods with non-overlapping segments in [21] (corresponding to "Non-overlapping" in the legend of the figure). In comparison with [21], when there is a code match, the proposed CERCD-I method actually performs filtering operation over the channel frequency responses, then takes absolute value of each output data sample of the filtering operation, and finally sums up all these absolute output data samples. In fact, the filtering operation is equivalent to a lowpass averaging operation over the channel responses. Here, by using a short window length (i.e., 3 in our algorithm demonstration), the proposed methods can better resist the adverse channel variation, because the consecutive subcarrier frequency responses within the short window length will be much more flatter than the much wider accumulation length in [21]. Since the proposed methods provide more average sum terms (due to overlapped use of $M_{i,m}(k)$ terms) with

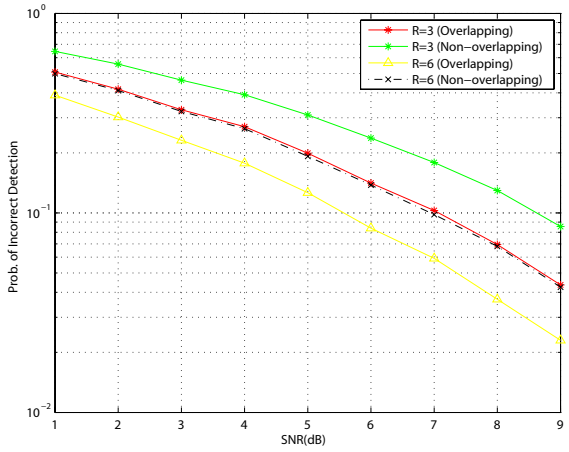

Fig. 8. The probability of the incorrect cell ID detection in a 6-path Rayleigh fading channel of the ITU-R vehicular A channel model ($f_{nd} = 0.1$).

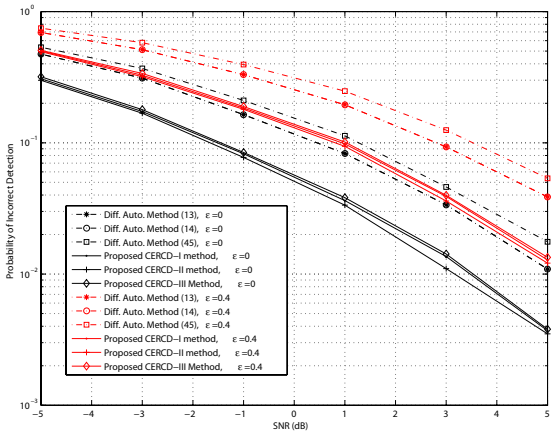

Fig. 9. The probability of the incorrect cell ID detection in a 6-path Rayleigh fading channel of the ITU-R vehicular A channel model..

small channel variations (due to short window length) than the method in [21] (with long window length and nonoverlapped use of $M_{i,m}(k)$ terms), higher integration gain can be obtained from the proposed methods than the method in [21], when the channel frequency responses vary noticeably over the subcarrier range, for examples, for non-flat channel responses or frequency selective channels. Hence, the proposed methods with overlapping $M_{i,m}(k)$s are more robust against non-flat channel conditions and burst error than the method with non-overlapping $M_{i,m}(k)$s in [21].

Fig. 9 and Fig. 10 show the simulation results under channel A and channel B with different residual frequency offsets (i.e., $\epsilon = 0$ and $\epsilon = 0.4$), respectively. Note that the "Diff. Auto. Method", appearing in the legends of those figures, means the conventional differential autocorrelation method. In the figures, the probabilities of the incorrect cell ID detection are compared. As shown, regardless of SNR and channel conditions, all the proposed methods exhibit better performances than the conventional differential autocorrelation methods whatever the residual frequency offset is.

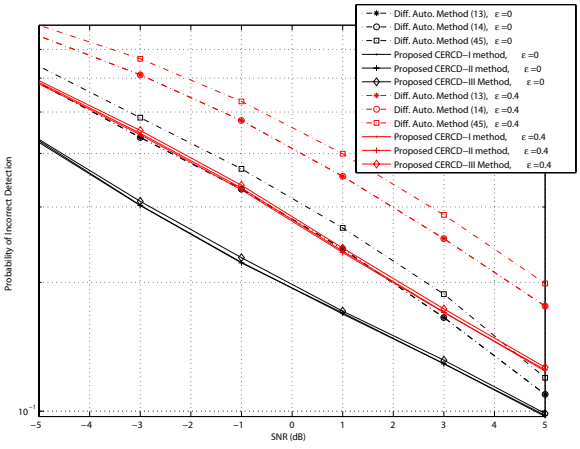

Fig. 10. The probability of the incorrect cell ID detection in a 6-path Rayleigh fading channel of the ITU-R vehicular B channel model.

Beside, in figures, the performance differences among the proposed methods are almost negligible. Let us first consider CERCD-I and CERCD-II methods. Although the performance of CERCD-II is conceptually better than CERCD-I as discussed in Section III, their difference is not much in the simulation, because a matched $|S_{i,m}(k)|$ with a large value in CERCD-I method automatically guarantees a large-value $|S_{i,m}(k)|^2$ in CERCD-II method, and vice versa. Therefore, both methods generate similar results in the maximum-value search process (i.e., $argmax$). Next, let us consider CERCD-I and CERCD-III methods. Since $||S_{i,m}(k)||$ of CERCD-III method is a simplified version of the absolute operation $|S_{i,m}(k)|$ of CERCD-I method and $||S_{i,m}(k)||$ is always larger than or equal to $|S_{i,m}(k)|$, a large matched $|S_{i,m}(k)|$ value in CERCD-I method also automatically guarantees a large matched $||S_{i,m}(k)||$ value in CERCD-III method, like in the comparison discussion between CERCD-I and CERCD-II methods. Hence, both methods also have very close performance. However, a small-value unmatched $|S_{i,m}(k)|$ in CERCD-I method does not necessarily imply a small-value $||S_{i,m}(k)||$ in CERCD-III method. In this case, it will cause performance degradation of CERCD-III method. As such, performance of CERCD-III is inferior but close to that of CERCD-I method.

For the conventional methods, the reason why the performance of the absolute operation $|(.)|$ in (13) is close to that of the square absolute operation $|(.)|^2$ in (14) is the same as explained in the comparison of CERCD-I and CERCD-II methods. Since conventional methods take the absolute value operation after the entire differential autocorrelation operation, i.e., $|\sum_{k=0}^{N-2} M_{i,m}(k)M_{i,m}^*(k+1)|$, the conventional method of (45) have larger performance differences from (13) and (14) than the differences of CERCD-III from CERCD-I and CERCD-II methods. As previously discussed, note that the conventional methods accumulate the $M_{i,m}(k)M_{i,m}^*(k+1)$ terms in the entire subcarrier range. Hence, conventional methods are subject to channel variations. On the other hand, the proposed methods are less influenced by channel variation effects, because the basic smoothing term of $|M_{i,m}(k) + M_{i,m}(k+1) + M_{i,m}(k+2)|$ is operated in a limited local range. Due to the much longer accumulation range than that of CERCD-III method, the approximation error of $||\sum_{k=0}^{N-2} M_{i,m}(k)M_{i,m}^*(k+1)||$ to $|\sum_{k=0}^{N-2} M_{i,m}(k)M_{i,m}^*(k+1)|$ will be much larger than the error between CERCD-I and CERCD-III methods. Hence, one can see a large difference between (45) and (13) or (14) than the difference between CERCD-III and CERCD-I or CERCD-II methods.

Next, we will discuss the performances of the conventional and proposed methods. For conventional methods, the basic accumulation term $M_{i,m}(k)M_{i,m}^*(k+1)$ in differential autocorrelation supposedly can cancel the channel phases of the k-th and $(k+1)$-th preamble subcarriers, given that $H(k) \approx H(k+1)$. As a result, $M_{i,m}(k)M_{i,m}^*(k+1)$ reduces to either $|H(k)|^2$ or $-|H(k)|^2$ regardless of whether there is a code match or not. When there is a code match, then all the $M_{i,m}(k)M_{i,m}^*(k+1)$ terms will produce the squared channel response magnitudes with the same sign. Then by accumulating all the $M_{i,m}(k)M_{i,m}^*(k+1)$ terms, i.e., $\sum_{k=0}^{N-2} M_{i,m}(k)M_{i,m}^*(k+1)$, one can obtain a significantly large absolute autocorrelation value (i.e., $|\sum_{k=0}^{N-2} M_{i,m}(k)M_{i,m}^*(k+1)|$ is approximately equal to $\sum_{k=0}^{N-2} |H(k)|^2$). On the other hand, when there is no code match, the signs of $M_{i,m}(k)M_{i,m}^*(k+1)$ will vary with k randomly so that one will obtain a much smaller $|\sum_{k=0}^{N-2} M_{i,m}(k)M_{i,m}^*(k+1)|$ value than the matched case. Since conventional methods assume equal channel responses at two consecutive preamble subcarriers, i.e., $H(k) \approx H(k+1)$, their performances will be poor if the channel variation is high and the phase difference between these two subcarriers' channel frequency responses will not be small so that one will not expect either $|H(k)|^2$ or $-|H(k)|^2$ value from $M_{i,m}(k)M_{i,m}^*(k+1)$. Under this condition the accumulation value of $|\sum_{k=0}^{N-2} M_{i,m}(k)M_{i,m}^*(k+1)|$ will be much less than the cases under small channel variations.

On the other hand, the proposed methods actually performs channel response smoothing operation, i.e., $S_{i,m}(k) = M_{i,m}(k) + M_{i,m}(k+1) + ... + M_{i,m}(k+R) = H(k) + H(k+1) + ... + H(k+R)$, when there is a code match. Thus, the proposed methods can obtain a large matched value of $\sum_{k=0}^{N-R} |S_{i,m}(k)|$. However, when there is no code match, value of $M_{i,m}(k) + M_{i,m}(k+1) + ... + M_{i,m}(k+R)$ can randomly be any one of the 2^R possible results (depending on k): $\pm H(k) \pm H(k+1) \pm ... \pm H(k+R)$. As such, it leads to a smaller mismatched value of $\sum_{k=0}^{N-R} |S_{i,m}(k)|$. Consequently, one can see that the proposed methods do not utilize the channel phase differential operations used by conventional differential autocorrelation methods, in the cell ID detection. Without relying on differential phase technique and assuming equal channel phases of two consecutive subcarriers, the proposed methods are less influenced by the channel response variations. Hence, the proposed methods have better performances than the conventional autocorrelation-based methods as illustrated in Fig. 9 and Fig. 10.

In addition, for reducing the computational complexities and further generalizing the optimization metrics, one can include a decimation factor d in the conventional and proposed

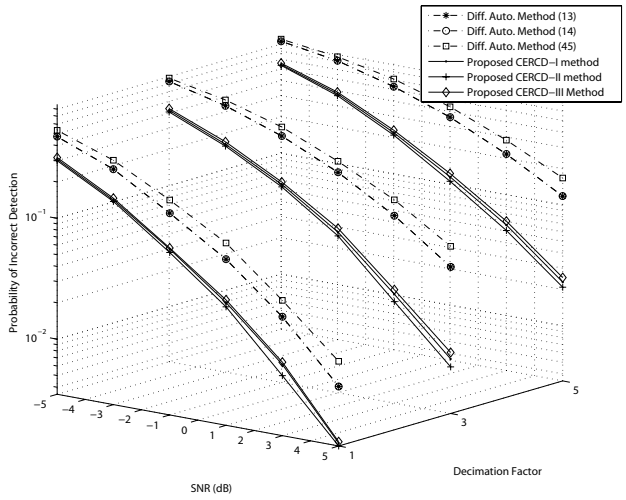

Fig. 11. The probability of the incorrect cell ID detection in a 6-path Rayleigh fading channel of the ITU-R vehicular A channel model, under different decimation factors, when $\epsilon = 0$ and $\tau = 4$.

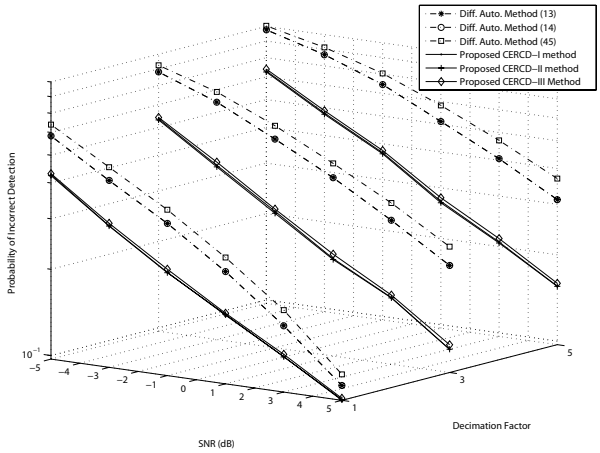

Fig. 12. The probability of the incorrect cell ID detection in a 6-path Rayleigh fading channel of the ITU-R vehicular B channel model, under different decimation factors, when $\epsilon = 0$ and $\tau = 4$.

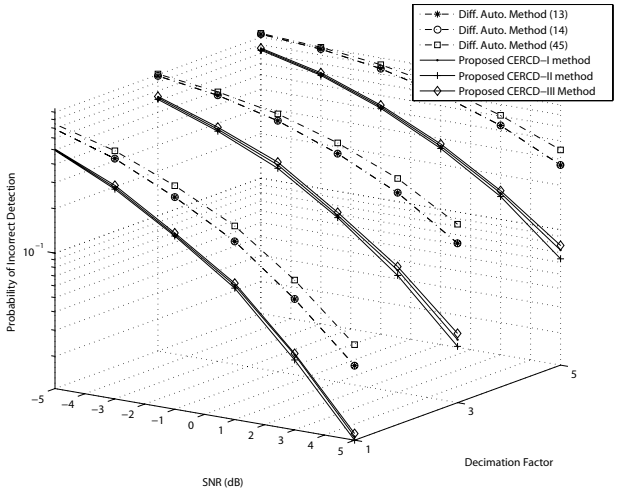

Fig. 13. The probability of the incorrect cell ID detection in a 6-path Rayleigh fading channel of the ITU-R vehicular A channel model, under different decimation factors, when $\epsilon = 0.4$ and $\tau = 4$.

methods as follows.

- Generalized Differential Autocorrelation Method of (13):

$$\hat{i} = \arg\max_{0\le m\le M-1} \quad |\sum_{k=0}^{\lfloor\frac{N-2}{d}\rfloor} M_{i,m}(k\times d) \times M^*_{i,m}(k\times d+1)|$$

- Generalized Differential Autocorrelation Method of (14):

$$\hat{i} = \arg\max_{0\le m\le M-1} \quad |\sum_{k=0}^{\lfloor\frac{N-2}{d}\rfloor} M_{i,m}(k\times d) M^*_{i,m}(k\times d+1)|^2$$

- Generalized Differential Autocorrelation Method of (45):

$$\hat{i} = \arg\max_{0\le m\le M-1} \quad \| \sum_{k=0}^{\lfloor\frac{N-2}{d}\rfloor} M_{i,m}(k\times d) M^*_{i,m}(k\times d+1) \|$$

- Generalized CERCD-I Method:

$$\hat{i}_I = \arg \max_{0\le m\le M-1} \sum_{k=0}^{\lfloor\frac{N-3}{d}\rfloor} |S_{i,m}(k\times d)|$$

- Generalized CERCD-II Method:

$$\hat{i}_{II} = \arg \max_{0\le m\le M-1} \sum_{k=0}^{\lfloor\frac{N-3}{d}\rfloor} |S_{i,m}(k\times d)|^2$$

- Generalized CERCD-III Method:

$$\hat{i}_{III} = \arg \max_{0\le m\le M-1} \sum_{k=0}^{\lfloor\frac{N-3}{d}\rfloor} \| S_{i,m}(k\times d) \|$$

Note that $\lfloor\ \rfloor$ is the floor function, the decimation factor d is a positive integer. As shown in the generalized methods, only one subcarrier out of every d subcarriers is included in the accumulation of optimization functions. Consequently, one can do the tradeoff between complexities and performances of those methods in practical applications.

Fig. 11 and Fig. 12 show the performances of the conventional and proposed methods when decimation factor $d = 1, 3, 5$, residual frequency offset $\epsilon = 0$, $R = 3$, and all the weighting coefficients $a_r = 1$. Note that the performances of the conventional and proposed methods when $d = 1$ in Fig. 11 and Fig. 12 are the same as in Fig. 9 and Fig. 10, respectively. In addition, regardless of decimation factors, Fig. 11 and Fig. 12 show that all the proposed methods have better performances than the conventional methods. Fig. 13 and Fig. 14 show the performances of those methods under vehicular A channel and vehicular B channel, respectively, when the residual frequency offset $\epsilon = 0.4$. In the presence of the residual frequency offset, similar observation to Fig. 11 and Fig. 12 are obtained. That is, all the proposed methods work well and have better performance than the conventional methods.

VII. Conclusion

Based on the proposed new metric and its two simplifications, three new non-coherent cell ID detection techniques and statistical analysis for cellular OFDM systems have been proposed in this work. All the proposed methods have better performances than the conventional methods. Especially, the complexity analysis and simulation results show that the proposed CERCD-III method has much lower complexity

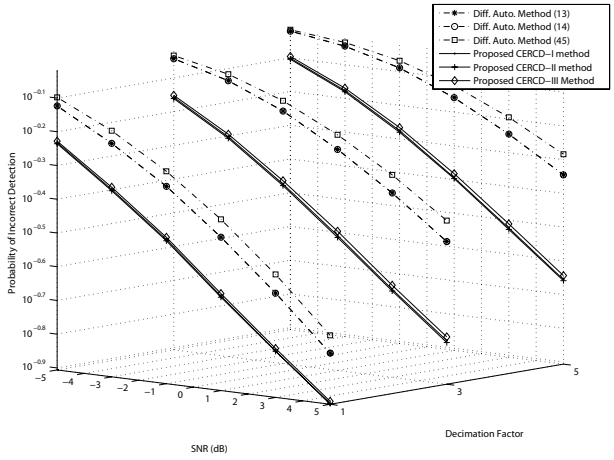

Fig. 14. The probability of the incorrect cell ID detection in a 6-path Rayleigh fading channel of the ITU-R vehicular B channel model, under different decimation factors, when $\epsilon = 0.4$ and $\tau = 4$.

and higher performance than the conventional methods. As a result, the proposed methods can be effectively applied to preamble-based OFDM systems in frequency-selective multipath channels. Furthermore, the new methods can be also easily extended to applications which need to identify a transmitted signal from a set of known reference signals.

REFERENCES

[1] C.-L. Chen and S.-G. Chen, "An efficient cell search algorithm for preamble-based OFDM systems," in *Proc. IEEE Personal, Indoor Mobile Radio Commun. (PIMRC)*, Sep. 2008, pp. 1–5.

[2] 3GPP, R1-062007, Texas Instruments, "Comparing hierarchical and non-hierarchical cell search," Aug. 2009.

[3] S. Nagata, Y. Kishiyama, M. Tanno, K. Higuchi, and M. Sawahashi, "Cell search time comparison using hierarchical and non-hierarchical synchronization channels in OFDM based evolved UTRA downlink," in *Proc. IEEE Vehicular Technology Conf. (VTC) Spring*, Apr. 2007, pp. 1239–1244.

[4] K. S. Kim, K. H. Chang, and S. W. Kim, "A preamble-based cell searching technique for OFDM cellular systems," in *Proc. IEEE Vehicular Technology Conf. (VTC)*, Oct. 2003, pp. 2471–2475.

[5] K. S. Kim, S. W. Kim, Y. S. Cho, and J. Y. Ahn, "Synchronization and cell-search technique using preamble for OFDM cellular systems," *IEEE Trans. Veh. Technol.*, vol. 56, no. 6, pp. 3469–3485, Nov. 2007.

[6] S. Nagata, Y. Kishiyama, M. Tanno, K. Higuchi, and M. Sawahashi, "Investigations of synchronization channel sequences in OFDM based evolved UTRA downlink," in *Proc. IEEE Vehicular Technology Conf. (VTC) Fall*, Sep. 2007, pp. 1390-1395.

[7] P. Cheng, Z. Zhang, X. Zhou, J. Li, and P. Qiu, "A study on cell search algorithms for IEEE 802.16e OFDMA systems," in *Proc. IEEE Wireless Commun. Networking Conf. (WCNC)*, Mar. 2007, pp. 1848–1853.

[8] J. W. Lee and Y. H. Lee, "Rapid cell search in OFDM-based cellular systems," in *Proc. IEEE Vehicular Technology Conf. (VTC)*, June 2005, pp. 1273–1277.

[9] H. Su, J. Zhang, and P. Zhang, "A preamble-based cell search scheme for OFDM cellular systems," in *Proc. IEEE Networking, International Conf. Systems International Conf. Mobile Commun. Learning Technologies (ICNICONSMCL)*, Apr. 2006, pp. 197–201.

[10] F. Berggren and B. M. Popovic, "A non-hierarchical cell search scheme," in *Proc. IEEE Wireless Commun. Networking Conf. (WCNC)*, Mar. 2007, pp. 2300–2304.

[11] P. A. Murugesa Pandian and S. Srikanth, "Low complexity cell search for mobile OFDMA system," in *Proc. IEEE International Conf. Signal Processing, Commun. Networking (ICSCN)*, Jan. 2008, pp. 189–193.

[12] S. B. Weinstein and P. M. Ebert, "Data transmission by frequency-division multiplexing using the discrete Fourier transform," *IEEE Trans. Commun.*, vol. 19, pp. 628–634, Oct. 1971.

[13] IEEE std 802.16-2004, IEEE Standard for Local and Metropolitan Area Networks-Part 16: Air Interface for Fixed and Mobile Broadband Wireless Access Systems, Oct. 2004.

[14] IEEE std 802.16e/D9, IEEE Standard for Local and Metropolitan Area Networks-Part 16: Air Interface for Fixed and Mobile Broadband Wireless Access Systems, June 2005.

[15] ETSI TR 101 112 V3.2.0, Universal Mobile Telecommunications System (UMTS); Selection Procedures for the Choice of Radio Transmission Technologies of the UMTS (UMTS 30.03 version 3.2.0), ETSI, Apr. 1998.

[16] F. C. Leone, L. S. Nelson, and R. B. Nottingham, "The folded normal distribution," *Technometrics*, vol. 3, no. 4, pp. 543–550, Nov. 1961.

[17] Y. R. Zheng and C. Xiao, "Simulation models with correct statistical properties for Rayleigh fading channels," *IEEE Trans. Commun.*, vol. 51, no. 6, pp. 920-928, June 2003.

[18] J. L. Rodgers and W. A. Nicewander, "Thirteen ways to look at the correlation coefficient," *American Statistician*, vol. 42, pp. 59–65, 1988. Y. R. Zheng and C. Xiao, "Simulation models with correct statistical properties for Rayleigh fading channels," *IEEE Trans. Commun.*, vol. 51, no. 6, pp. 920–928, June 2003.

[19] V. S. Abhayawardhana and I. J. Wassell, "Residual frequency offset correction for coherently modulated OFDM systems in wireless communication," in *Proc. IEEE Vehicular Technology Conf. (VTC) Spring*, 2002, vol. 2, pp. 777–781.

[20] J. Park, *et al.*, "Performance analysis of channel estimation for OFDM systems with residual timing offset," *IEEE Trans. Wireless Commun.*, vol. 5, no. 7, pp. 1622–1625, July 2006.

[21] Y.-P. E. Wang and T. Ottosson, "Cell search in W-CDMA," *IEEE J. Sel. Areas Commun.*, vol. 18, no. 8, pp. 1470–1482, Aug. 2000.

[22] P. Cheng, Z. Zhang, X. Zhou, J. Li, and P. Qiu, "A study on cell search algorithms for IEEE 802.16e OFDMA systems," in *Proc. IEEE Wireless Commun. Networking Conf. (WCNC)*, Mar. 2007, pp. 1848–1853.

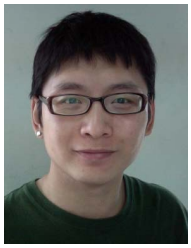

Chih-Liang Chen was born in Tainan, Taiwan. He received the B.S.E.E. degree from National Chung Hsing University, Taiwan, in 2005. During 2009, he was a visiting scholar in the Department of Electrical Engineering and Computer Science, the University of Michigan, USA. He is currently a Ph.D. candidate in the Department of Electronics Engineering and Institute of Electronics, National Chiao Tung University, Taiwan. His research interests include digital signal processing, synchronization, channel estimation, and equalization.

Sau-Gee Chen received his B.S. degree from National Tsing Hua University, Taiwan, in 1978, and the M.S. and Ph.D. degrees in electrical engineering from the State University of New York at Buffalo, NY, in 1984 and 1988, respectively. During 2003 and 2006, he was director of the Institute of Electronics, Department of Electronics Engineering, National Chiao Tung University, Taiwan. Currently, he is a professor at the same organization. His research interests include digital communication, multi-media computing, digital signal processing, and VLSI signal processing. He has published more than 70 conference and journal papers, and holds several US and Taiwan patents.